

On the Asteroidal Population of the First-Order Jovian Resonances

D. Nesvorný and S. Ferraz-Mello

Universidade de São Paulo, Instituto Astronômico e Geofísico, Av. Miguel Stefano 4200, 04301 São Paulo, Brazil
E-mail: david@orion.iagusp.usp.br

Received February 21, 1997; revised June 30, 1997

The frequency map analysis was applied to the fairly realistic models of the 2/1, 3/2, and 4/3 jovian resonances and the results were compared with the asteroidal distribution at these commensurabilities. The presence of the Hecuba gap at the 2/1 and of the Hilda group in the 3/2 is explained on the basis of different rates of the chaotic transport (diffusion) in these resonances. The diffusion in the most stable 2/1-resonant region is almost two orders in magnitude faster than the diffusion in the region which accommodates the Hildas. In the 2/1 commensurability there are two possible locations for long-surviving asteroids: the one centered at an eccentricity of 0.3 near the libration stable centers with small libration amplitude and the other at a slightly lower eccentricity with a moderate libration amplitude ($\sim 90^\circ$). Surprisingly, all asteroids observed in the 2/1 resonance (8 numbered and multi-opposition objects in Bowell's catalog from 1994) occupy the moderate-libration area and avoid the area in a close vicinity of the libration stable centers. Possible explanations of this fact were discussed. Concerning the 4/3 resonance, the only asteroid in the corresponding stable region is 279 Thule, in spite of the fact that this region is almost as regular (although not as extensive) as the one where the Hilda group in the 3/2, with 79 members, is found. © 1997 Academic Press

Key Words: asteroids; resonances; frequency map analysis.

1. INTRODUCTION

It has been suggested by Ferraz-Mello (1994) from the analysis of the maximum Lyapunov exponents, that the chaotic diffusion is much faster in the 2/1, than in the 3/2 jovian resonance and that this faster diffusion is the main reason why the original population of the 2/1 resonance was reduced during the solar system evolution. As a consequence, the Hecuba gap was formed at the 2/1 commensurability while a large number of asteroids survived in the 3/2 resonance now belonging to the Hilda group.

We have tested this hypothesis using the frequency map analysis of Laskar (1988) (see also the recent review: Laskar 1996), adapted for the particular problem of jovian resonances (Nesvorný and Ferraz-Mello 1997). This method allowed us to estimate the diffusion rates of an

extensive set of trajectories in both resonances. Moreover, we have included the 4/3 resonance in our study.

Figure 1 shows the basic characteristics of the first-order mean-motion resonances in the averaged, planar circular three-body model. The Hamiltonian of this model is of two degrees of freedom and is separable. Considering the $(p + q)/p$ resonance, the integral of motion $N = \sqrt{\mu a} [(p + q)/p - \sqrt{1 - e^2}]$ (μ is the product of the gravitation constant and the mass of the Sun, a and e are the semi-major axis and eccentricity of an asteroid, inclination $i = 0$) divides the phase space into the manifolds $N = \text{const}$ on which the motion takes place. The trajectories on $N = \text{const}$ can be described by the pair $(\sigma = ((p + q)/q)\lambda_1 - p/q\lambda - \varpi, e)$, where λ_1 and λ are the mean longitudes of Jupiter and an asteroid and ϖ is the asteroid longitude of perihelion.

As an example, Fig. 2 shows two sets of trajectories with $N = 0.457$ and $N = 0.51$ for the 3/2 resonance. For $N = 0.457$ and the asteroid inside the resonance, σ librates around zero and e oscillates approximately around 0.22. The point $(\sigma, e) = (0, 0.22)$ is the stable stationary solution (libration center) and the set of these points for different N (for instance, $(\sigma, e) = (0, 0.4)$ for $N = 0.51$) forms the so-called pericentric branch of the stable stationary solutions which is, in Fig. 1, shown in a plane (a, e) as the full line denoted by h.

The thick line for $N = 0.457$ in Fig. 2 is the separatrix which separates the libration and the circulation of σ . The points where it crosses $\sigma = 0$ (approximately at $e = 0.14$ and 0.27 for $N = 0.457$) can give a useful estimate of the resonance width. They are shown for different N as the full lines in the plane (a, e) denoted by s1 and s2 in Fig. 1 for the 3/2 resonance.

The same computation was done for all studied first-order resonances, and their pericentric branches of the libration centers and separatrices are shown in Fig. 1 as the full lines.

For all resonances, the topology of trajectories on $N = \text{const}$ changes above a certain limit where the possibility of collision with Jupiter appears. This happens roughly at the dashed line in Fig. 1 above which the aphelion of the

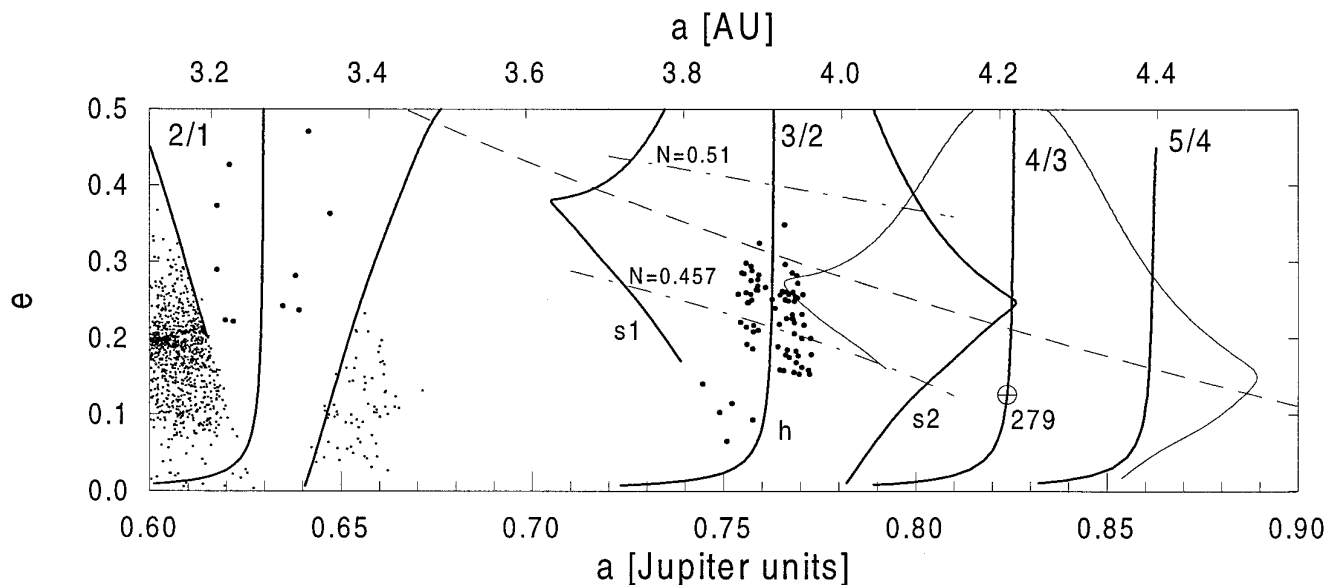


FIG. 1. The first-order jovian resonances. The full lines are the pericentric branches of the stable stationary solutions (denoted by *h* for the 3/2 resonances) and separatrices (denoted by *s1* and *s2*). The collisions with Jupiter are possible above the dashed line (however, the resonant asteroids are phase-protected from collisions). Two levels of $N = 0.457$ and $N = 0.51$ are shown for the 3/2 (dotted and dashed lines), one under and the other above the collision limit. See Fig. 2 for the topology of trajectories on these levels in the circular model. The observed resonant and near-resonant asteroids are shown by large and small dots, respectively. 279 Thule is the only asteroid in the 4/3 (\oplus). See the text for details.

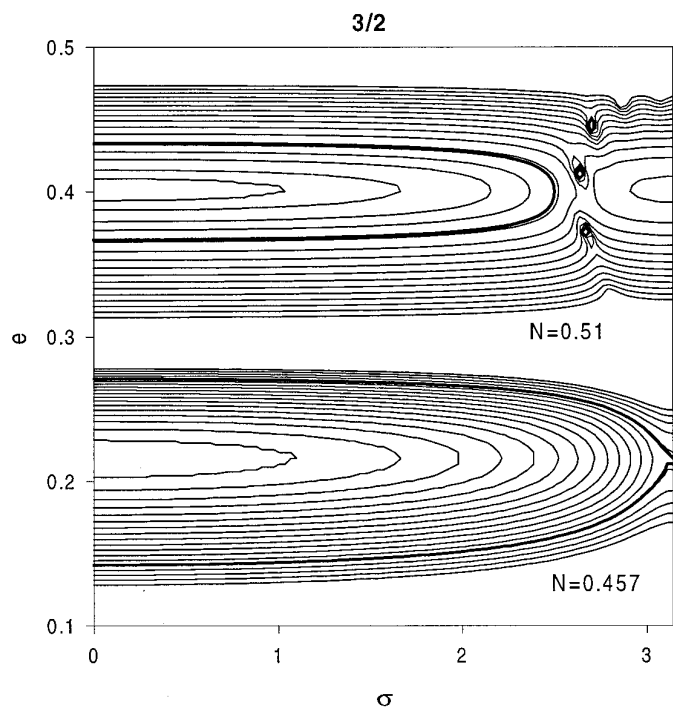


FIG. 2. The composite of two sets of trajectories: $N = 0.457$ and $N = 0.51$, in the averaged planar circular three-body model of the 3/2 resonance.

asteroid orbit lies outside Jupiter's orbit. The separatrices do not exist for higher eccentricities and the full lines above the dashed line correspond to the trajectories with the maximum libration amplitude which are still phase-protected from the collision (see the next two paragraphs).

In Fig. 2, the set of trajectories with $N = 0.51$ (which is above the Jupiter-crossing limit) is given. The two libration regions are the pericentric one with librations around $(\sigma, e) = (0, 0.4)$ and the one which encircles the new stable point at $(\sigma, e) = (\pi, 0.4)$. They are separated by the singularity of the perturbing function at about $\sigma = 2.7$ where close approaches with Jupiter happen. The asteroids, which come too close to this collision region, get, in the non-averaged model, an impulse from Jupiter which is often sufficient to remove them from the resonance.

The width of the resonance above the Jupiter-crossing limit thus refers to the largest libration trajectory (around $\sigma = 0$) which avoids the collision. As an example, this reference trajectory is plotted as the thick line in Fig. 2 for $N = 0.51$.

The cataloged asteroids inside the resonances and in their proximity were numerically integrated with four outer planets to the reference plane $\sigma = 0$ and $\varpi - \varpi_1 = 0$ so that their position corresponds to the position of the separatrices in Fig. 1 (see Morbidelli *et al.* (1995) for a more detailed discussion of the correct comparison of the separatrices and the asteroidal positions). There are 10 objects in the 2/1 (the neighboring non-resonant asteroids

are printed as very small dots—only the pericentric librators reasonably far from the borders of the resonance are regarded as resonant in this paper), 79 members of Hilda group in the 3/2, and only 279 Thule in the 4/3. Each point in Fig. 1 corresponds to one asteroid, strictly speaking, to its first crossing of the reference plane. Those asteroids for which the first crossing happens with $\sigma < 0$ appear on the left side of the pericentric branch and others with $\sigma > 0$ appear on the right side.

An additional note concerns the overlap of resonances 3/2 and 4/3 which can be seen in Fig. 1. This overlap is not as deep as can be erroneously inferred from the figure, since the left separatrix of the 4/3, which seems to come very close to the libration centers of 3/2 and interfere with the Hildas, is in fact on a different plane (defined by $\sigma = 4\lambda_1 - 3\lambda - \varpi = 0$) than the characteristics represented for the 3/2 (defined by $\sigma = 3\lambda_1 - 2\lambda - \varpi = 0$). In other words, Fig. 1 is only a graphical composite of reference planes for different resonances. However, as we will see later, the overlap actually does exist and generates a large scale chaos around $a = 0.8$ (in units 5.203 AU).

The following sections are devoted to the description of the diffusion portraits—the local estimates of the chaotic diffusion on selected manifolds in the phase-space. First we treat individually the 2/1, 3/2, and 4/3 resonances and then, in the last section, we present their comparison.

2. THE 2/1 RESONANCE

2.1. Diffusion Portraits

The two rectangles in Fig. 3 define two sets of initial conditions in the representative plane $i = 0$, $\sigma = 2\lambda_1 - \lambda - \varpi = 0$, $\varpi - \varpi_1 = 0$, and $\Omega - \Omega_1 = 0$ in the usual notation of Keplerian variables (the index 1 denotes the quantities of Jupiter). Each initial condition was integrated in the restricted four-body model with Jupiter and Saturn on their real orbits using the symmetric multi-step method (Quinlan and Tremaine 1990). The system Sun–Jupiter–Saturn was propagated by a parallel integration of the three-body model. The low-pass filter of Quinn *et al.* (1991) was applied to the variable $e \exp i\varpi$ ($i = \sqrt{-1}$), which was then decomposed into harmonics using the FMFT (frequency modified Fourier transform) method of Šidlichovský and Nesvorný (1997) in two subsequent time intervals of 2×10^5 yr with an overlap of 10^5 yr in the case of the low-eccentricity set and two intervals of 4×10^5 yr with an overlap of 2×10^5 yr for the high-eccentricity set. This doubling of times was done in order to avoid the effect of near-harmonics in the high eccentricities (Nesvorný and Ferraz-Mello 1997) where motion timescales are longer (Michtchenko and Ferraz-Mello 1995).

The absolute value of the relative change of the leading frequency f_ϖ in the spectra (normalized to 10^5 years) was

used as a measure of the local diffusion speed. The black squares in Fig. 3 correspond to the trajectories with $\delta f_\varpi > 10^{-2}$ and the small crosses to $10^{-2} > \delta f_\varpi > 10^{-3}$ (the big gray squares forming the central gray area in high eccentricities and the gray areas at both sides of the rectangle, delimiting the high-eccentricity set, are highly chaotic orbits which quickly escaped from the resonance). The rest, which was left blank, is the most stable area with $\delta f_\varpi < 10^{-3}$.

The figure, centered at the 2/1 resonance, reveals several already known characteristics of this resonance. The low-eccentricity chaos caused by an overlap of the low-order secondary resonances was discovered by Giffen (1973) (see Lemaître and Henrard 1990). The chaos in high eccentricities ($e > 0.4$) originates from the secular resonances ν_5 and ν_6 (Morbidelli and Moons 1993) and, together with the chaos near separatrices, encloses the chaotic, but comparatively more stable area at approximately $0.25 < e < 0.4$ in the center (A), which extends to a wider range in eccentricity when the amplitude of libration increases (B). The stable area B has a low-eccentricity V-shaped prolongation at roughly $a = 0.638$ going as low as $e = 0.1$. The typical relative frequency change normalized to 10^5 yr ranges here from 10^{-2} to slightly less than 10^{-3} .

The areas A and B are separated by a narrow ridge of faster diffusion, which can be identified with the secular resonance ν_{16} . This resonance forms an arc which touches the complex of secondary resonances at about $e = 0.2$ (see also Fig. 5).

An additional detailed study showed that the most stable and compact regions in the resonance, where on average $\delta f_\varpi < 10^{-3}$, are (1) centered at $e = 0.3$ and $a = 0.63$ and (2) between 0.635 and 0.641 in semi-major axis and between 0.18 and 0.23 in eccentricity. This second region has a counterpart on the left-hand side of the resonance (at about $a = 0.62$ and $e = 0.27$) due to the fact that each resonant trajectory traverses the considered plane $\sigma = 0$ twice: once with $\sigma < 0$ on the left-hand side and once with $\sigma > 0$ on the right-hand side. The above are the places where one should most likely expect to find asteroids (with low inclinations) lucky enough to survive for a long time inside the resonance.

In Fig. 4, δf_ϖ , smoothed by means of a 10-points moving average, is shown for two sets of initial conditions. The thick line corresponds to $a = 0.64$ and $i = 5^\circ$, and traverses the region B; the thin line corresponds to $a = 0.63$ and $i = 5^\circ$, and crosses A. The most stable regions where $\delta f_\varpi < 10^{-3}$ are clearly visible.

This result confirms the existence of the region with slow chaotic diffusion found by Morbidelli (1996) (our region B), which is, as we will see in the next section, associated to the four long-living resonant asteroids. In Morbidelli's integrations, only one initial condition was placed in our region A (his No. 21). The corresponding asteroid survived 1 Gyr in the resonance.

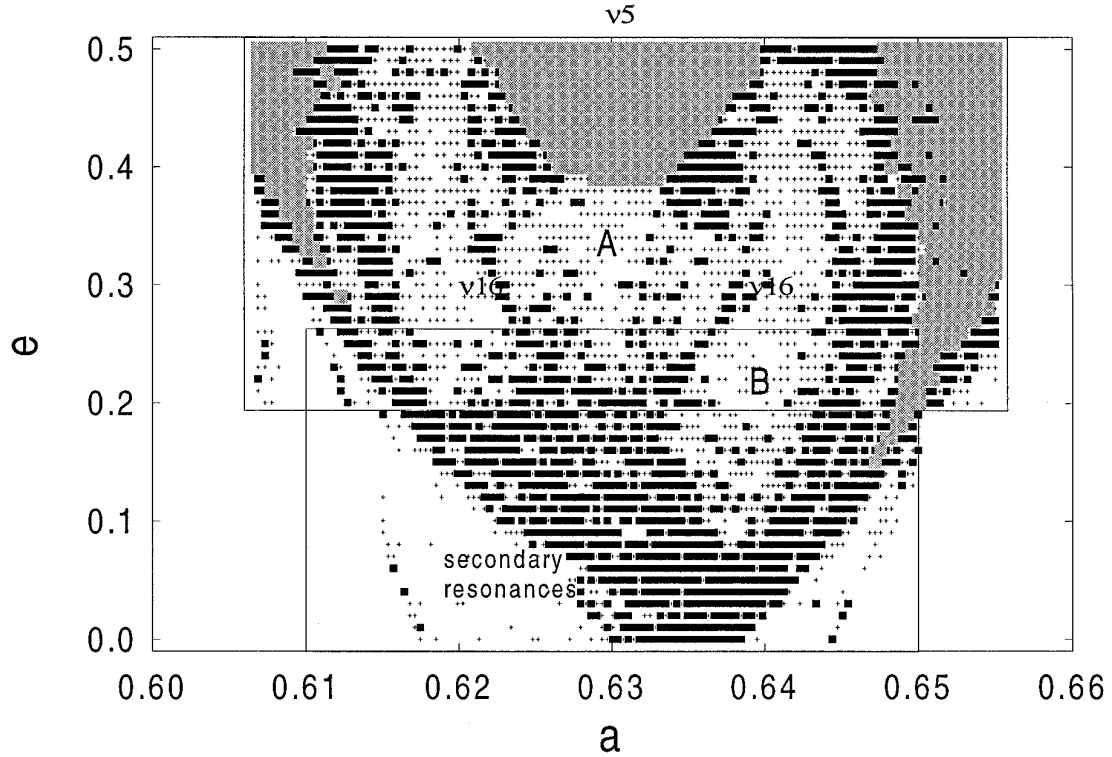


FIG. 3. The diffusion portrait of the 2/1 resonance in a representative plane with $i = 0$. Black squares correspond to $\delta f_{\varpi} > 10^{-2}$ in 10^5 yr, small crosses to $10^{-2} > \delta f_{\varpi} > 10^{-3}$, and voids to $\delta f_{\varpi} < 10^{-3}$. The gray area corresponds to highly chaotic escape orbits.

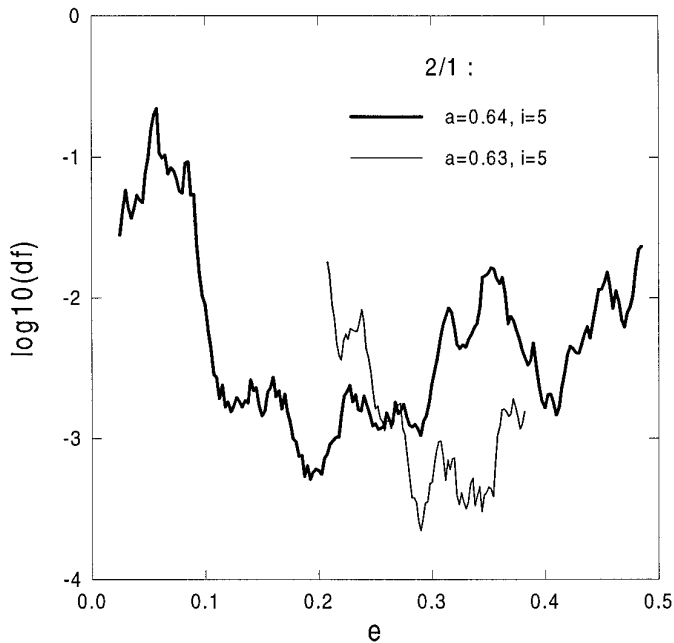


FIG. 4. δf_{ϖ} over 10^5 yr smoothed by means of a 10-points moving average for $a = 0.63$ and $a = 0.64$ (in units 5.203 AU). $i = 5^\circ$ in both cases.

At least for the sake of a qualitative estimate of the diffusion effect over 1 Gyr we may assume a random walk of the trajectory in the frequency space and that the mean square displacement is roughly proportional to the time. Hence, the average relative frequency change over 1 Gyr may be expected to be some 100 times larger than the estimates over 10^5 yr given above. This means a less than 10% frequency change in the most stable regions and changes as large as 100% in the region covered by black squares. In the first case, the change is sufficiently small and would probably allow some asteroids to stay in one of the larger and compact stable areas mentioned in the previous paragraph, for very long time intervals, of the order of 10^9 yr (this is the actual meaning of word “stable” as used in this article: the stable region is the one in which a significant portion of asteroids should survive 10^9 yr). In the second case, it can be claimed, as the corresponding region is formed by interconnected parts, that significant transitions may occur. A trajectory originating in the secondary resonances complex with a small libration amplitude may find the connection with the gray, fast-escape regions along the separatrices and leave the resonance. In the following, we will discuss another existing connection, and thus, another possible escape path from the secondary resonances complex, outside the plane $i = 0$.

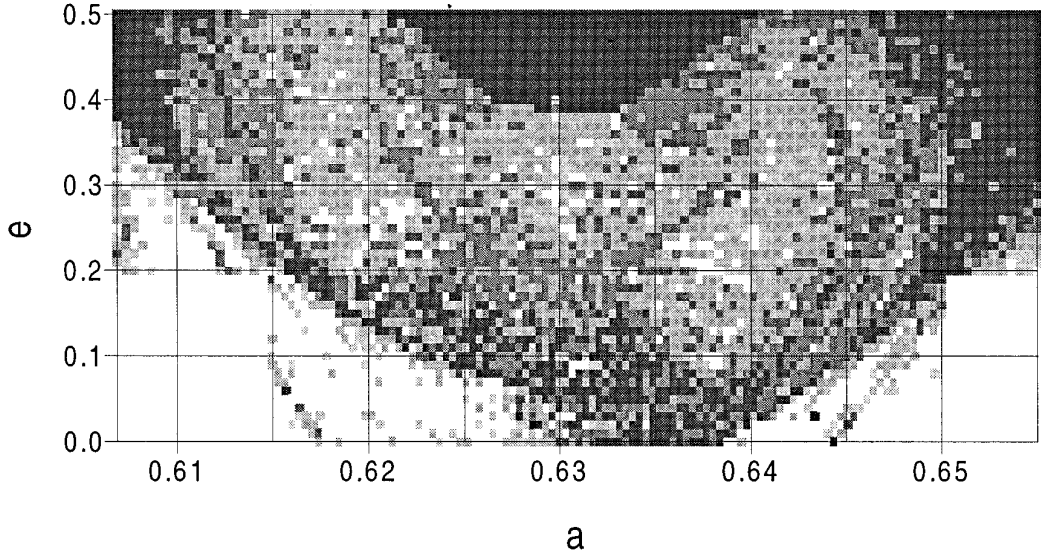


FIG. 5. The gray-scale coding of the same diffusion portrait as in Fig. 3. The five levels of gray ranks are defined by $\delta f_{\varpi} = 10^{-3.5}, 10^{-3}, 10^{-2},$ and 10^{-1} . The most regular (the brightest) area is where $\delta f_{\varpi} < 10^{-3.5}$ and the most chaotic (the darkest) area corresponds to $\delta f_{\varpi} > 0.1$ and to escaping trajectories.

Figure 5 is another view of the same diffusion portrait as in Fig. 3. The coding is a gray scale showing the most stable regions (with the smallest frequency change) as bright and the regions of fast diffusion as dark. The five levels of the gray scale are spanning several orders in magnitude of the frequency change. It ranges from 10^{-6} outside the resonance (10^{-3} in the most stable area in the resonance) to the very fast transitions in the complex of the secular resonances.

The plane (e, i) with fixed $a = 0.63$ and $a = 0.64$ is shown in Fig. 6. The coding is the same as in Fig. 3. The chaos in the low eccentricities (secondary resonances complex) is separated from the high-eccentricity chaos (secular resonances complex) by a barrier of less intense diffusion centered at about $e = 0.3$ for $a = 0.63$ and $e = 0.2$ for $a = 0.64$. One can observe the important role of the secular resonance ν_{16} (computed numerically and marked by Δ) for the transitions to high eccentricities. For $a = 0.63$, ν_{16} merges with the secondary resonances and there exists no path between low (< 0.25) and high eccentricities, but, for $a = 0.64$, the ν_{16} resonance forms the connection of significant transitions at $i > 30^\circ$. This was already observed in the numerical integrations of Wisdom (1987) and studied by Henrard *et al.* (1995), where it was named “bridge.” Any orbit in the secondary resonances complex can pass over this bridge and reach the secular resonances complex, from which it is removed typically by a close encounter with Jupiter.

Thus, the absence of real asteroids in the low-eccentricity region is well understood and, at present, the problem is to explain what happens in the central region $0.625 < a <$

0.635 and $0.25 < e < 0.4$ (marked A in Fig. 3) and at about $a = 0.64$ for eccentricities $0.1 < e < 0.3$, in the narrowing area going as high as 25° in inclination (marked B).

The indicator of the chaotic diffusion used in this section was the relative change of the frequency of the perihelion longitude (δf_{ϖ}). Another option, the frequency of the longitude of node f_{Ω} , or more precisely, the leading frequency in the spectra of $i \exp \Omega$, was tested. The results were basically the same, with a partial difference in the region $e > 0.3$ for low inclinations ($i < 10^\circ$) in Fig. 6 (left) ($a = 0.64$), where the rate of the chaotic diffusion indicated by δf_{Ω} was slightly higher, typically on the order of 10^{-2} .

2.2. The Observed Asteroids

In Fig. 7 we compare the actual asteroidal distribution to the diffusion portrait at $i = 0$. As in Fig. 3, the black squares denote the initial conditions with $\delta f_{\varpi} > 10^{-2}$, the gray area is the fast escaping trajectories, and the void area represents the relatively stable trajectories (but remember that almost everywhere in the resonant region $\delta f_{\varpi} \geq 10^{-3}$). The separatrices and the locus of the pericentric libration orbits shown here as the thick lines were computed in the circular three-body model.

The numbered and multi-opposition asteroids from Bowell’s catalog—version updated at the end of 1994 (Bowell *et al.* 1994)—were integrated with the four outer planets and their positions were registered (dots) when simultaneously $|\sigma| < 10^\circ$ and $|\varpi - \varpi_1| < 10^\circ$. The striking concentration at the boundary of the left separatrix is the Themis family.

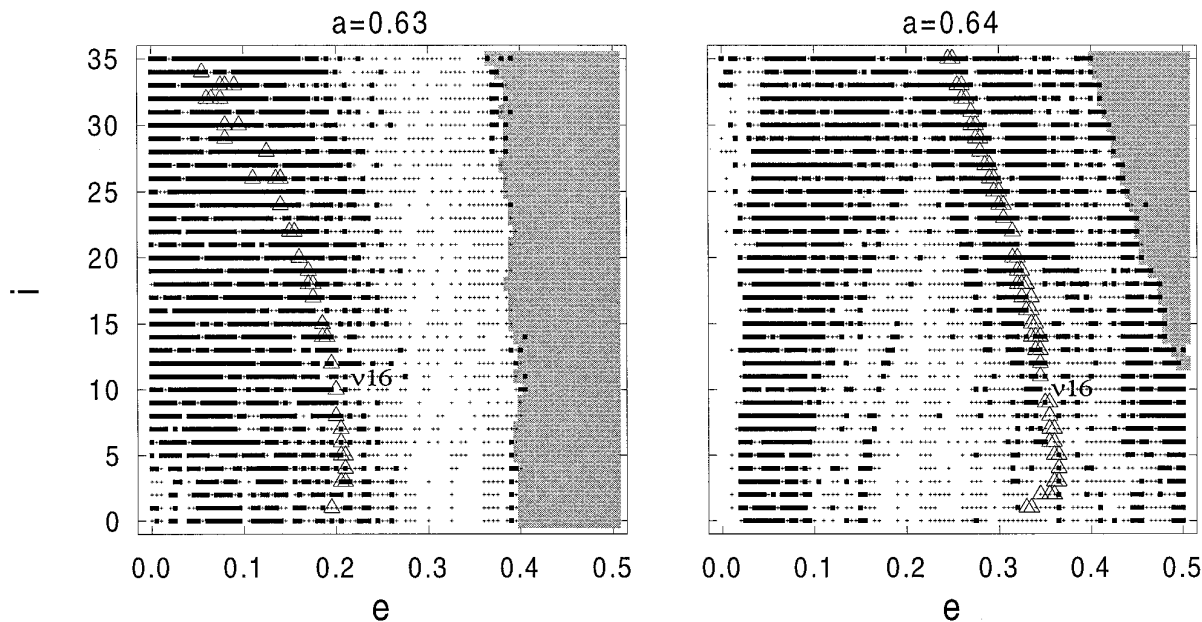


FIG. 6. The diffusion portrait of the 2/1 resonance in the plane (e, i) for $a = 0.63$ (left) and $a = 0.64$ (right). The secular resonance ν_{16} is marked by Δ . Coding as in Fig. 3.

The resonant asteroids found (\oplus) were further integrated until the additional condition $\sigma > 0$ was fulfilled and thus they appeared on the right-hand side of the pericentric stable points (in this account, Fig. 7 differs to what has been done in Fig. 1, where each resonant asteroid was followed only until $|\sigma| < 10^\circ$ regardless of the sign of σ). Including two single-opposition asteroids, their number is rounded to 10. They are 1362, 1921, 1922, 3688, 3789, 4177, 1975SX, 1990TH7, 1981EX11, and 1993SK3 numbered in

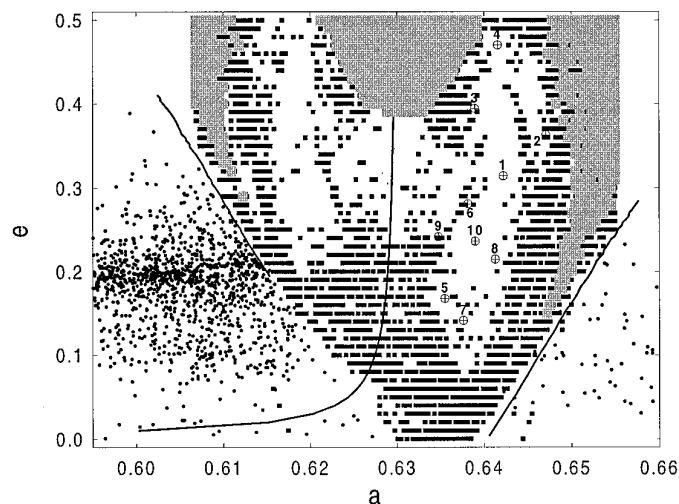


FIG. 7. The distribution of the real asteroids compared to the diffusion portrait of Fig. 3.

the figure, from 1 to 10, respectively. In Table I, the osculating elements of the resonant asteroids for $\sigma = 0$ ($\sigma > 0$) and $\varpi - \varpi_1 = 0$ are given.

In this projection, most of the resonant asteroids avoid the compact, strongly chaotic regions and appear in the relatively more stable area, which would be a nice verification of what should be expected, but some of them have high inclinations and are actually on unstable trajectories. This is not the case of 5, 7, 8, and 10 which have $i < 5^\circ$ and project well into the base of the stable barrier in Fig. 6 (see also Fig. 14 in the last section), but surely it is the case of 3, which is at inclinations above 35° on a strongly chaotic orbit. The asteroids numbered 1, 2, 6, and 9 are at

TABLE I
The Elements of Asteroids in the 2/1 Resonance

No.	Name	a/JU	a/AU	e	i
1	1362 Griqua	0.6422	3.342	0.314	23.9
2	1921 Pala	0.6471	3.367	0.363	18.8
3	1922 Zulu	0.6390	3.325	0.394	38.1
4	3688 Navajo	0.6416	3.338	0.470	2.9
5	3789 Zhongguo	0.6355	3.307	0.168	1.6
6	4177 1987 SS1	0.6381	3.320	0.281	18.2
7	1975 SX	0.6376	3.318	0.141	3.2
8	1990 TH7	0.6413	3.337	0.214	0.9
9	1981 EX11	0.6348	3.303	0.241	18.2
10	1993 SK3	0.6390	3.325	0.236	2.1

Note. $JU = 5.203 AU$.

eccentricities from 0.18 to 0.24, number 9 at the edge of the stable area (see Fig. 14) and the others inside the secular resonances complex. Our prolonged numerical integrations show escapes of these asteroids from the resonance in the intervals of the order of 10^7 yr. The case 4 is on strongly chaotic orbit at low inclinations.

These results were compared to the recent numerical integrations of Morbidelli (1996). The elements of the resonant asteroids given in our Table I cannot be directly compared to Morbidelli's Table I due to the opposite signs of σ for several asteroids. However, an additional check showed a good agreement for all objects. The small differences in this comparison probably account for our 10° interval of freedom for the angles or a slightly different definition of our and Morbidelli's "proper resonant elements."

The four asteroids: 3789 Zhongguo (5), 1975SX (7), 1990TH7 (8), and 1993SK3 (10), which are in the stable region at low eccentricities in Fig. 6, are exactly the asteroids identified by Morbidelli (1996) as resonant objects in the region stable over more than 1 Gyr. From the other three asteroids, which did not escape in Morbidelli's 38-Myr integration, two objects (4111 1987SS1 (6) and 1981EX11 (9)) are at the border of the regular region (see Fig. 14) close to the secular resonance ν_{16} . The third asteroid, 1362 Griqua (1), and the three unstable asteroids over 38 Myr studied by Morbidelli are already deep in the secular resonances complex.

As we can see, there are no asteroids in the central area A although this region is even slightly more stable than B. This similarity of the diffusion rates in the regions A and B and the difference of their asteroidal population is puzzling. We will discuss this subject in the next section.

2.3. The Stable Regions A and B

Michtchenko and Ferraz-Mello (1997) suggested that the lack of asteroids in the region A may be due to particular short-periodic perturbations of the Jupiter-Saturn pair. These planets are, as is generally known, near the mutual $5/2$ mean-motion resonance. The angle of the so-called "great inequality" circulates with the period of about 880 yr and this period is very sensitive to a small change of the orbits. If, at some time in the history of the solar system, this period was only slightly more than 400 years, which corresponds to a relative change in the mean semi-major axis of Jupiter (or Saturn) of a mere 10^{-4} , then the resonance with the asteroidal libration might have happened.

Figure 8 shows the libration period of σ in the $2/1$ resonance. It is about 430 yr in A and less than 400 yr in B. In Ferraz-Mello and Michtchenko (1997) simulations in which the period of $5/2$ Jupiter-Saturn resonance was roughly 430 yr, the resonance-induced chaos in A expelled the asteroids in a timescale roughly on the order of 10^8 yr;

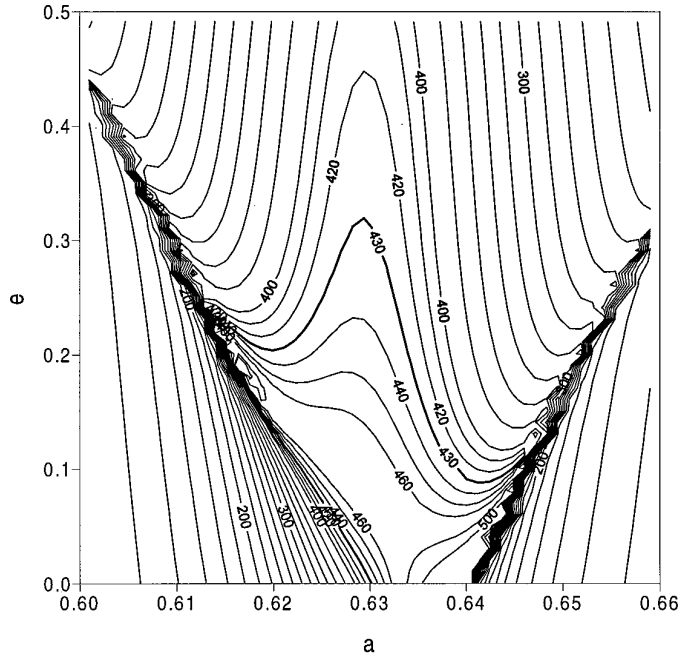


FIG. 8. The libration period (in years) in the $2/1$ resonance (circular problem).

the population of B was less affected. It was suggested in Michtchenko and Ferraz-Mello (1997) that the depletion of A is a consequence of the diffusion accelerated by the Jupiter-Saturn great inequality terms.

Figure 9a shows the detail of the diffusion portrait in Fig. 3: region A and the counterpart of B on the left side of the pericentric libration centers. First, we tested whether the regularity of A is perhaps an artifact of the dynamical model restricted to the perturbations of only Jupiter and Saturn. Figure 9b is the portrait made with four outer planets. Apparently, there is no big difference to Fig. 9a and the model with only two planets represents well the reality.

Figure 9c is the model with the real orbit of Jupiter and a slightly changed orbit of Saturn so that the $5/2$ great inequality period was about 430 yr. This modification generated stronger chaos especially in higher eccentricities affecting both A and B regions. The stable regions became much smaller. One can see that the short-periodic terms may be really important for an explanation of the internal population of the $2/1$ resonance and surely deserves further study. By comparing Figs. 8 and 9c it is seen that the effect of Jupiter-Saturn short-periodic terms is not limited to the very domain where the libration period is 430 yr, but spreads to a large neighborhood of this domain.

The non-resonant asteroidal group, at the lower limit of the left separatrix in Fig. 7, is the well-known Themis family, which has been recently studied as a product of primordial body disruption and its interaction with the

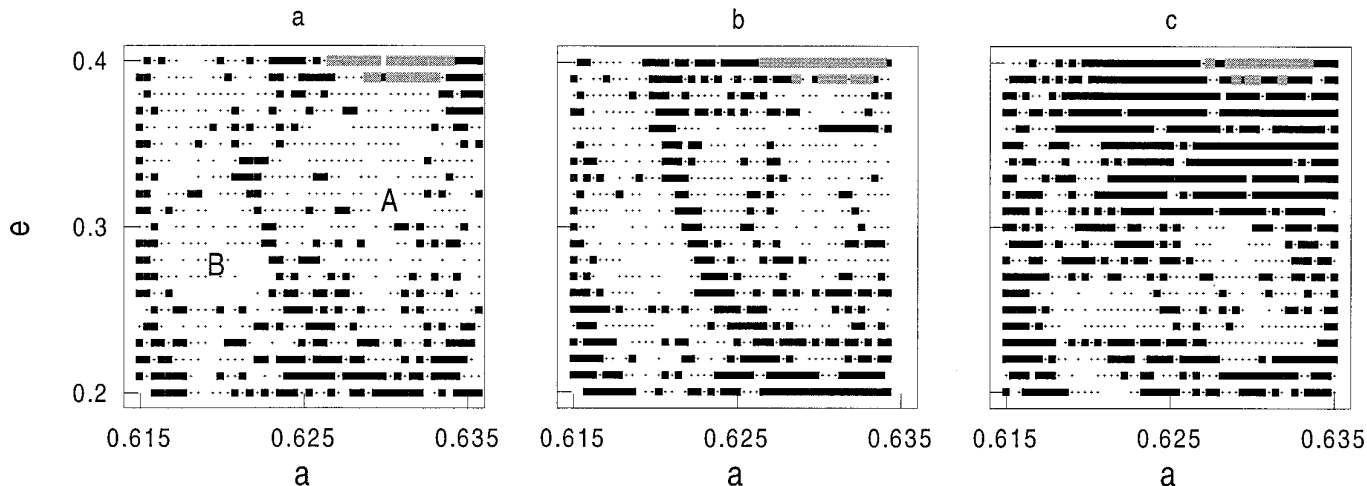


FIG. 9. (a) A detail of the diffusion portrait shown in Fig. 3. (b) The same area but computed in the model with the perturbations of four outer planets. (c) Again the model with only Jupiter and Saturn, but a slightly changed initial condition of Saturn (see text).

resonance by Morbidelli *et al.* (1996). It is one of the most numerous asteroidal families and is considered to be the remnant of a collision event more than 1 Gyr ago (Marzari *et al.* 1995).

Morbidelli (1996) suggested that the breakup of the parent body of the Themis family injected many fragments into the resonance. Therefore, the region B, which is near the supposed breakup position, might have been refilled with small asteroids, while the region A need not be reached by Themis ejecta, since it is much deeper in the resonance. This idea is supported by several facts (see Morbidelli 1996) and may contribute to the explanation of the A versus B problem. However, in our analysis, the stability of the region A seems to be sufficient to maintain some primordial objects for the time intervals on the order of few Gyr, and since no asteroid is observed there now, another dynamical mechanism might have been in work, as, for instance, the small drift of the resonance suggested by Michtchenko and Ferraz-Mello (1997).

3. THE 3/2 RESONANCE

In Fig. 10, we show the diffusion portraits of the 3/2 resonance in two planes: (a, e) with $i = 0$ (left) and (e, i) with $a = 0.768$ (right). The experiment (two perturbing planets) and the coding are the same as in the case of the 2/1 resonance, but since the diffusion is slower here, it is more convenient to reserve the small crosses for $10^{-2} > \delta f_{\omega} > 10^{-4}$. The thick line shows the locus of the pericentric libration orbits of the circular problem.

The numbered and multi-opposition Hildas (63 + 16 = 79 members) were, as in the case of the 2/1 resonance, integrated roughly to the planes $\sigma = 3\lambda_1 - 2\lambda - \varpi = 0$ ($\dot{\sigma} > 0$) and $\varpi - \varpi_1 = 0$, and plotted as circles.

Several facts can be noted in Fig. 10: The central region of the 3/2 resonance is much more regular than that of the 2/1 resonance. Here, the whole area of $i < 15^\circ$ centered at $e = 0.25$ exhibits much slower diffusion than anywhere in the 2/1 resonance. The asteroids of Hilda group are located in this central stable area of the 3/2 resonance. The diffusion over 10^5 yr is $\delta f_{\omega} < 10^{-4}$ here, which would qualitatively mean less than a 10^{-2} change in 1 Gyr, which is apparently not sufficient for substantial transitions in the phase space. Consequently, the observed asteroidal population should be dynamically primordial.

The five asteroids seen in Fig. 10 (left) in low eccentricities: 334, 1256, 4196, 1981EF48, and 1985QX4 were omitted in the plot $a = 0.768$ since they are far from the chosen plane and their projection to this plane would be misleading. Although the secondary resonances are present in the low eccentricities, they are narrower for $i = 0$ here than in the 2/1 resonance and do not overlap (as shown by Michtchenko and Ferraz-Mello, 1995), which allows these five asteroids to survive on relatively stable orbits.

As in the case of the 2/1 resonance, we have computed the diffusion portraits in the model with four outer planets. This did not bring any substantial change to Fig. 10 and proved that the diffusion rates calculated in the model with only Jupiter and Saturn approximate well the reality.

An additional question concerns the effect of a slight orbital shift of Jupiter or Saturn on the diffusion in the 3/2 resonance. As we have seen before, even a negligibly small shift (say 10^{-4} relative change of Jupiter's semi-major axis) may seriously affect the period of the short periodic terms originating from the mutual Jupiter–Saturn 5/2 resonance and may dramatically change, through a resonance with the asteroid's libration period, the diffusion rate in the 2/1 asteroidal resonance (Fig. 9c).

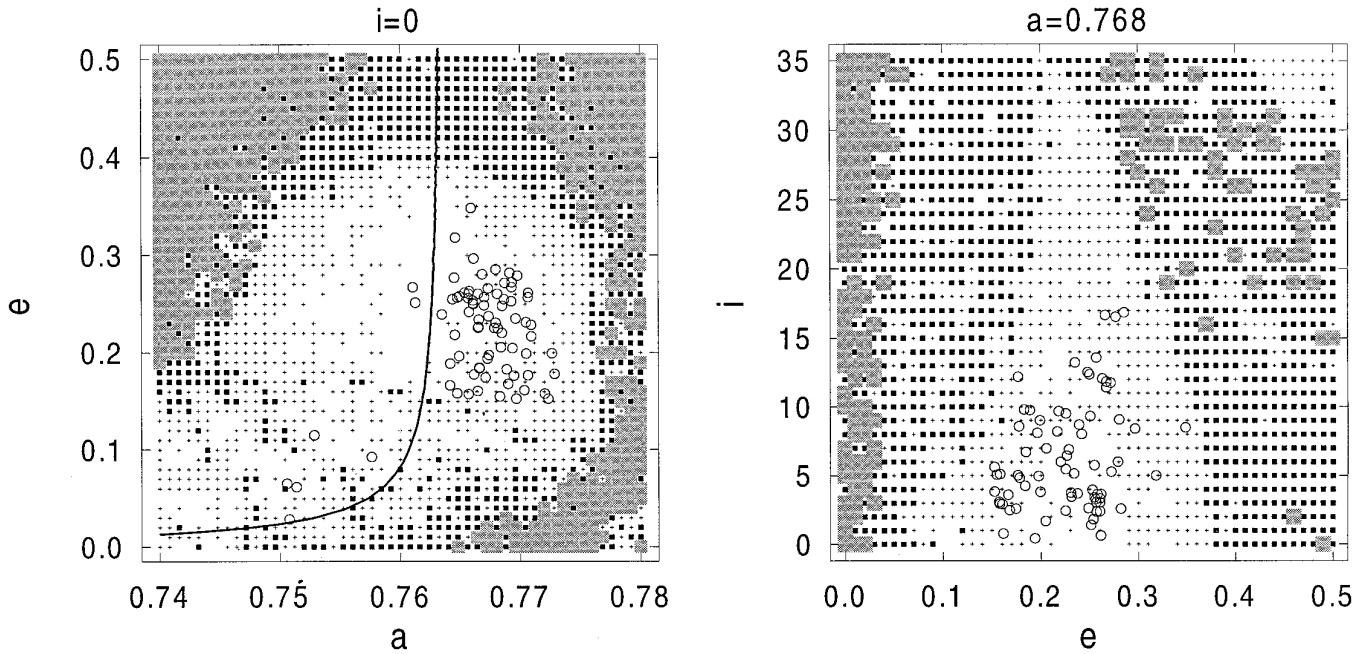


FIG. 10. The Hilda group and the diffusion portraits of the 3/2 resonance at $i = 0$ (left) and $a = 0.768$ (right). Black squares correspond to $\delta f_{\text{res}} > 10^{-2}$ in 10^5 yr, small crosses to $10^{-2} > \delta f_{\text{res}} > 10^{-4}$ and voids to $\delta f_{\text{res}} < 10^{-4}$. The gray area corresponds to highly chaotic escape orbits.

Figure 11 shows the libration period in the 3/2 resonance computed in the planar circular three-body model. It is significantly shorter than in the case of the 2/1 resonance (Fig. 8): for the majority of Hildas the libration period

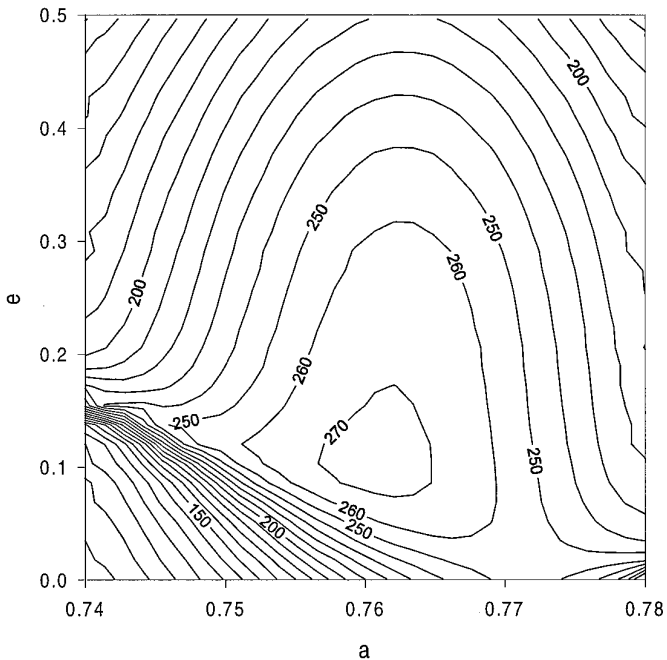


FIG. 11. The libration period (in years) in the 3/2 resonance (circular problem).

ranges from 250 to 270 yr. Consequently, if the resonance with the period of the great-inequality angle is to be assured, one must place the Jupiter–Saturn pair farther from their mutual resonance than in the case studied for the 2/1 asteroidal resonance: the great-inequality period should be about 260 yr instead of the actual 880 yr.

The effect of such a shift on the diffusion portraits in Fig. 10 was tested in several examples and found to be very small. Although a systematic study of this subject is necessary, we believe that the short-periodic perturbation terms resulting from the great inequality do not influence, even if its period is conveniently adjusted, the diffusion in the 3/2 resonance. The possible explanation may be based on the fact that the amplitudes of these perturbations are small when Jupiter and Saturn are farther from the mutual resonance. Hence, the short-period perturbations are small when the period is 260 yr; the resonance with the libration in 3/2 is weak and does not cause any significant acceleration of the diffusion.

4. THE 4/3 RESONANCE

The diffusion portraits of the 4/3 resonance are shown in Fig. 12. The two planes are (a, e) with $i = 0$ (left) and (e, i) with $a = 0.824$ (right). The experiment (two perturbing planets) and the coding is the same as before. Small crosses denote the initial conditions where $10^{-2} > \delta f_{\text{res}} > 10^{-4}$ and the thick line is the locus of the pericentric libration orbits.

The regular region is apparently smaller than in the case

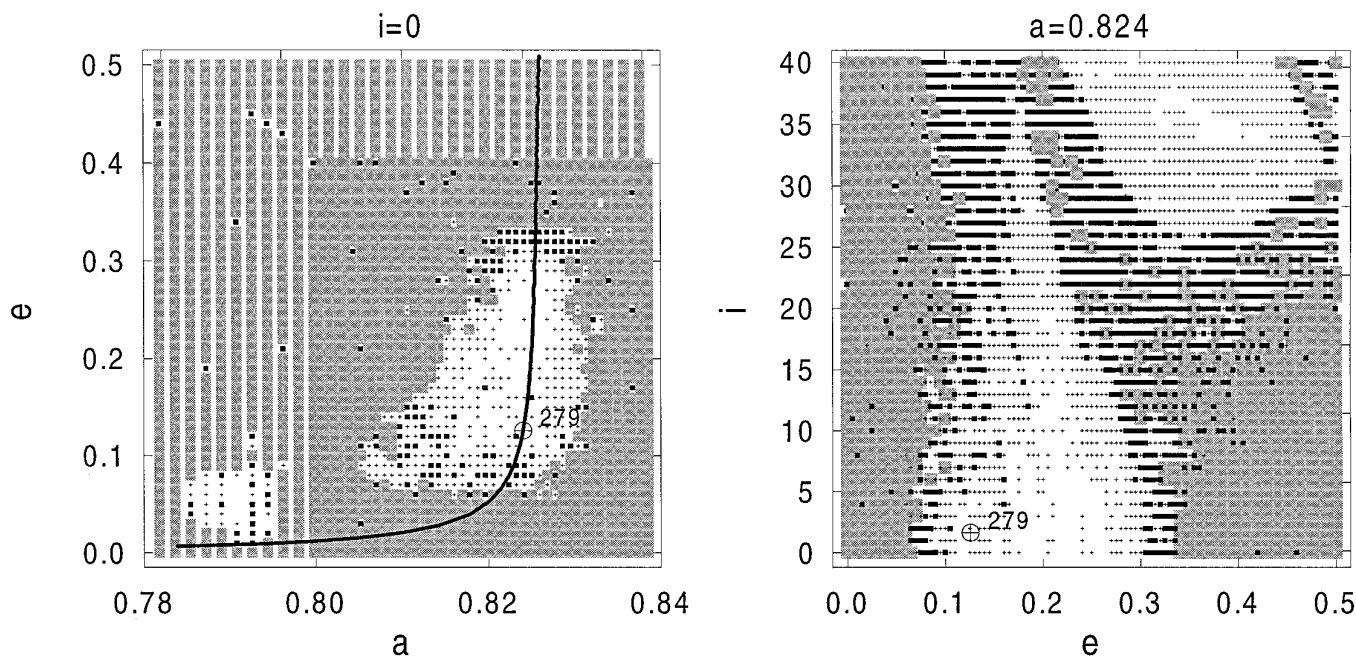


FIG. 12. The diffusion portraits of the 4/3 resonance at $i = 0$ (left) and $a = 0.824$ (right). Coding as in Fig. 10.

of the 3/2 resonance. For low inclinations, it surrounds the locus of pericentric libration orbits between 0.1 and 0.3 in eccentricity. The small regular island at $a = 0.79$ and $e = 0.05$ (left) quickly disappears with the increasing inclination and in the larger regular island centered at $e = 0.38$ and $i = 35^\circ$ (right) ω librates (Kozai resonance).

The diffusion portraits suggest that the resonant area might host a larger primordial population since the stability of the central area is comparable to that of the 3/2 resonance. But there is only one observed asteroid inside the resonance: 279 Thule. It was integrated to the plane $\sigma = 4\lambda_1 - 3\lambda - \varpi = 0$ and $\varpi - \varpi_1 = 0$, and placed at the bottom limit of the central stable area ($\delta f_\varpi < 10^{-4}$) in the low inclinations.

Figure 13 shows the mean frequency change normalized to 10^5 yr along the line at $a = 0.824$ and $i = 3^\circ$ which crosses the most regular region of the 4/3 resonance. The thick line in Fig. 13 is the frequency change computed in the model with Jupiter and Saturn, and the thin line is the frequency change computed in the model with four outer planets. It is remarkable that the diffusion rate increases almost by one order of magnitude when all perturbations of the outer planets are included, but even in this fairly realistic model the mean frequency change over 10^5 yr is under the level 10^{-4} in the large region between 0.17 and 0.26 in eccentricity. The diffusion is very slow there and, in our model, probably not sufficient for removing the primordial population.

This result was supported by several numerical integrations of 1.5×10^8 years with four outer planets with aster-

oids initially in the central regular area. The osculating elements did not exhibit any notable chaotic transitions and the stability of motion over much longer time periods may be expected. The objects initially placed in the Kozai

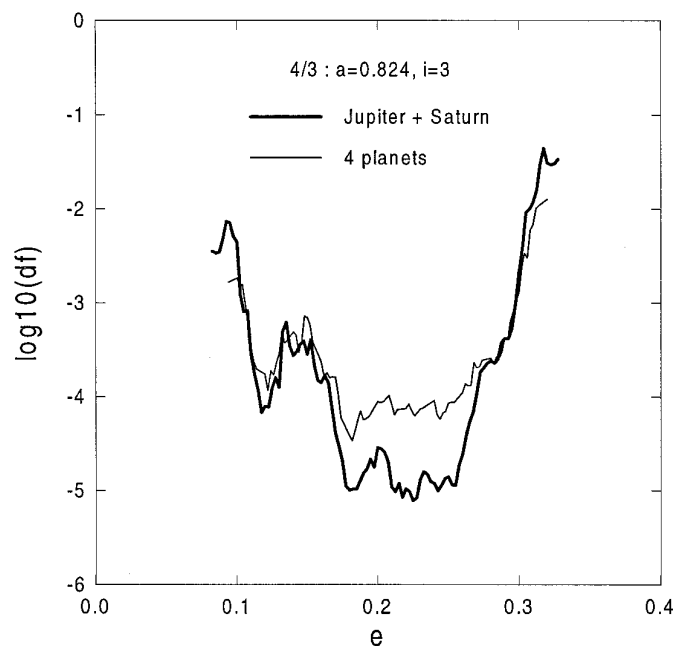


FIG. 13. Mean frequency change over 10^5 years in the 4/3 resonance: $a = 0.824$ and $i = 3^\circ$. Thick line is the problem with two perturbing planets and the thin line is the problem with the perturbations of four outer planets.

resonance at about $e = 0.38$ and $i = 35^\circ$ (Fig. 12 (right)) also had a very regular behavior in these integrations.

Similarly to the 2/1 and 3/2 resonances, the influence of a slight change of Jupiter's and Saturn's orbits on the diffusion in the 4/3 resonance was studied. It was found negligible in all investigated examples.

5. CONCLUSIONS

The observed characteristics of the 2/1 and 3/2 resonances and their internal asteroidal population are summarized in Fig. 14. The coding of the frequency portraits is the same in both figures (the small crosses correspond to $10^{-2} < \delta f_{\varpi} < 10^{-3}$) in order to permit the direct comparison of the diffusion in both resonances. The diffusion in the 3/2 resonance is, in general, much slower than in the 2/1.

Figure 15 shows the mean frequency change normalized to 10^5 yr along the horizontal lines in Fig. 14, at $i = 5^\circ$ and a similar line at $a = 0.824$ and $i = 3^\circ$ in the 4/3 resonance. In this resonance, δf_{ϖ} was computed only for non-escaping trajectories with initial e approximately between 0.08 and 0.32.

The lines of initial conditions were chosen so as to cross the most stable regions of the resonances. The Hilda group is located mostly in the interval where the frequency variation is under the level 10^{-4} . There is no such stable region in the 2/1 resonance and this difference in diffusion rates

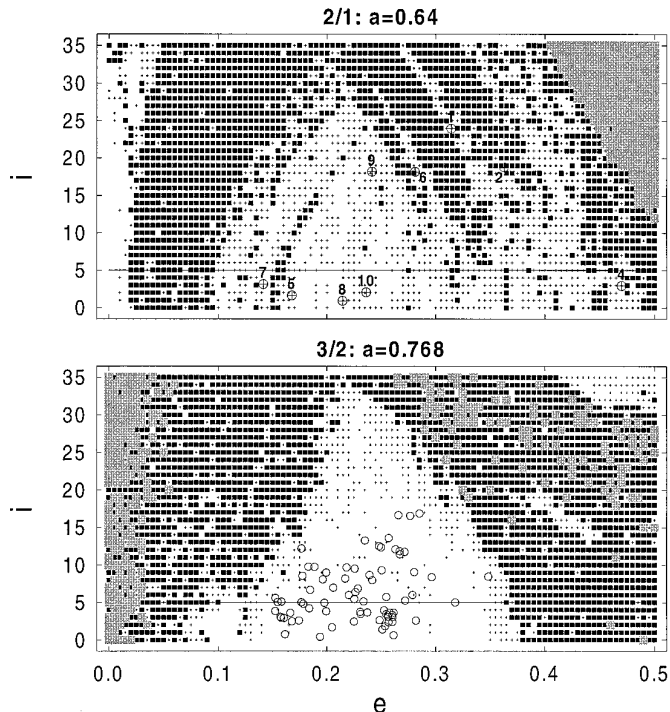


FIG. 14. (e, i) plane in the 2/1 resonance (top) and in the 3/2 resonance (bottom), with equal codings as in Fig. 3. Two perturbing planets.

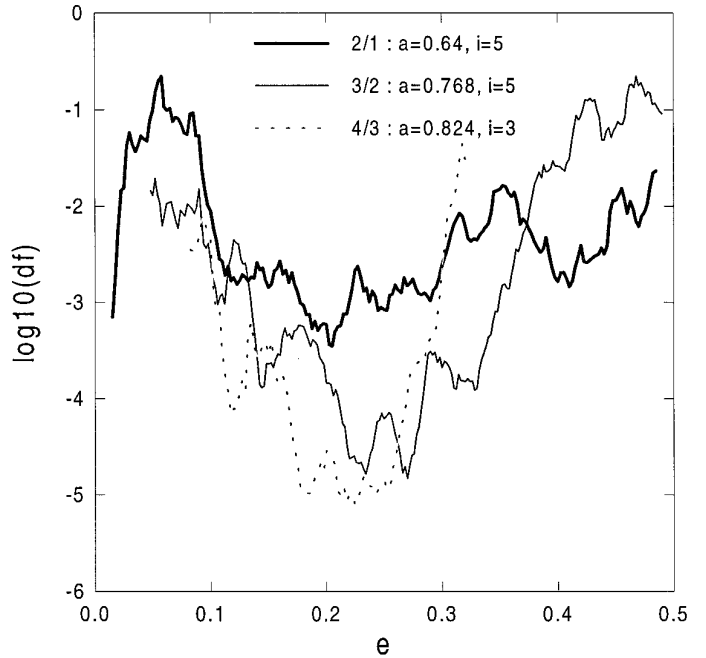


FIG. 15. Mean frequency change over 10^5 yr in the 2/1 ($a = 0.64$) and 3/2 ($a = 0.768$) resonances ($i = 5^\circ$ in both cases). The dashed line is the 4/3 resonance: $a = 0.824$ and $i = 3^\circ$. The model is with two perturbing planets.

may, indeed, explain the puzzling difference investigated for a long time between the populations of two most prominent first-order resonances in the asteroidal belt.

Moreover, the line of initial conditions $a = 0.824$ and $i = 3^\circ$ clearly demonstrates the degree of regularity of the central region of the 4/3 resonance. In the interval $0.15 < e < 0.25$, the change of f_{ϖ} is even lower than in the 3/2 resonance (in the model with Jupiter and Saturn only).

We have shown that the obtained diffusion portraits in the model with the perturbations of Jupiter and Saturn is sufficiently realistic in both the 2/1 and 3/2 resonances. Conversely, in the 4/3 resonance, the diffusion is accelerated when including the perturbations of all outer planets (Fig. 13). However, the central region of 4/3 preserves a high degree of regularity. This fact suggests that many primordial asteroids might survive there but only one, 279 Thule, is observed now. As the stability of the central region of the 4/3 resonance was confirmed by the long-term integrations, some explanation for the lack of the observed asteroids should be searched. Several conjectures may be offered (difference in primordial populations, collisional removal, resonance sweeping, etc.), but we would not like to enter into detailed discussion here.

Moreover, we have investigated the influence of the possible, very small shift of Jupiter's and Saturn's orbits. This shift does not affect the diffusion rates in the 3/2 and 4/3 resonances. In the case of 2/1, the resonance between

the asteroid librations and the short-periodic harmonics (with a conveniently adjusted period) originating from the great inequality led to the order of magnitude acceleration of the diffusion. If, sometime in the history of the solar system, Jupiter and Saturn were slightly more distant from their mutual $5/2$ mean-motion resonance, so that the period was about a half of its actual value, the process of asteroid ejection from the $2/1$ resonance was much more effective.

The difference in the asteroidal populations of the A and B regions in the $2/1$ resonance was discussed (Fig. 7). It is possible that, long after the primordial asteroids were removed from the resonance, the asteroids now present in B originated from the collision event which gave rise to the Themis family about 1 Gyr ago.

ACKNOWLEDGMENTS

The financial support of FAPESP (Research Foundation of the State of São Paulo) is acknowledged.

REFERENCES

- Bowell, E., K. Muinonen, and L. H. Wasserman 1994. A public-domain asteroid orbit database. In *Asteroids, Comets, Meteors* (A. Milani *et al.*, Eds.), pp. 477–481. Kluwer, Dordrecht.
- Ferraz-Mello, S. 1994. Dynamics of the asteroidal $2/1$ resonance. *Astron. J.* **108**, 2330–2337.
- Ferraz-Mello, S., and T. Michtchenko 1997. Orbital evolution of asteroids in the Hecuba gap. In *The Dynamical Behavior of Our Planetary System* (R. Dvorak *et al.*, Eds.), pp. 377–384. Kluwer, Dordrecht.
- Giffen, R. 1973. A study of commensurable motion in the asteroid belt. *Astron. Astrophys.* **23**, 387–403.
- Henrard, J., N. Watanabe, and M. Moons 1995. A bridge between secondary and secular resonances inside the Hecuba gap. *Icarus* **115**, 336–346.
- Laskar, J. 1988. Secular evolution of the Solar System over 10 million years. *Astron. Astrophys.* **198**, 341–362.
- Laskar, J. 1996. Introduction to frequency map analysis. In *Proceedings of the NATO Advanced Study Institute 3DHAM95*, Kluwer, Dordrecht, in press.
- Lemaître, A., and J. Henrard 1990. On the origin of chaotic behavior in the $2/1$ Kirkwood gap. *Icarus* **83**, 391–409.
- Marzari, F., D. Davis, and V. Vanzani 1995. Collisional evolution of asteroid families. *Icarus* **113**, 168–187.
- Michtchenko, T. A., and S. Ferraz-Mello 1995. Comparative study of the asteroidal motion in the $3/2$ and $2/1$ resonances with Jupiter. I. Planar model. *Astron. Astrophys.* **303**, 945–963.
- Michtchenko, T. A., and S. Ferraz-Mello 1997. Escape of asteroids from the Hecuba gap. *Planet. Space Sci.*, in press.
- Morbidelli, A. 1996. The Kirkwood gap at the $2/1$ commensurability with Jupiter: New numerical results. *Astron. J.* **111**, 2453–2461.
- Morbidelli, A., and M. Moons 1993. Secular resonances in mean motion commensurabilities: The $2/1$ and $3/2$ cases. *Icarus* **102**, 316–332.
- Morbidelli, A., V. Zappalà, M. Moons, A. Cellino, and R. Gonzi 1995. Asteroid families close to mean motion resonances: Dynamical effects and physical implications. *Icarus* **118**, 132–154.
- Nesvorný, D., and S. Ferraz-Mello 1997. Chaotic diffusion in the $2/1$ asteroidal resonance. *Astron. Astrophys.* **320**, 672–680.
- Quinlan, G. D., and S. Tremaine 1990. Symmetric multistep methods for the numerical integration of planetary orbits. *Astron. J.* **100**, 1694–1700.
- Quinn, T. R., S. Tremaine, and M. Duncan 1991. A three million year integration of the Earth's orbit. *Astron. J.* **101**, 2287–2305.
- Šidlichovský, M., and D. Nesvorný 1997. Frequency modified Fourier transform and its application to asteroids. *Celest. Mech. and Dynam. Astron.* **65**, 137–148.
- Wisdom, J. 1987. Chaotic dynamics in the Solar System. *Icarus* **72**, 241–275.